KAWASAKI STEEL TECHNICAL REPORT
No.39 (October 1998)
Electrical Steel

Shear Capacity of CFT Column and Precast Wall Structure

Takashi Iwasaki, Shinya Inaoka, Yukio Murakami, Koji Morita

Synopsis :
The CFT-PCa earthquake resistant wall structure developed for application in the construction of middle-to high-rise multi-family housing complexes consists of concrete filled tubes (CFT) columns and precast reinforced concrete (PCa RC) earthquake resistant walls. Cyclic shear bending tests were conducted on this structure using one-third scaled three-storied models which utilized two different types of connections between the columns and walls. The models of the first type, referred to as "concrete filled type" models, were constructed such that a plate girder was embedded in each wall. After the girders plates are bolted to the columns, the vertical space left between the columns and walls was filled with concrete. Models of the second type, known as "bolt type" models, were built such that each wall was embedded with a T-bar on which reinforcing bars were welded. The T-bars were then bolted to gussets fitted to the columns. Tests confirmed that both types of models demonstrate sufficient strength and energy absorption capacity. Studies of design formulas served to determine that strength can be estimated assuming such structures as an arch mechanism plus inter-story arch mechanism in the case of the concrete filled type of model and as a truss mechanism plus inter-story arch mechanism in the case of the bolt type of model structure.

The body can be viewed from the next page.

Shear Capacity of CFT Column and Precast Wall Structure*


Takashi Iwasaki
Staff Deputy Manager, Building Engineering Dept., Construction Engineering Div.


Shinya Inaoka
Staff Assistant Manager, Construction Materials Business Planning Dept., Construction Materials Center

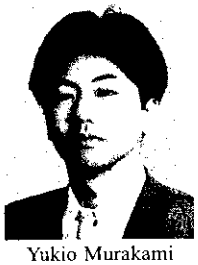
Yukio Murakami
Structural Res. Labs., Construction Materials Center


Koji Morita
Prof., Dr. Eng., Department of Design Engeineering, Faculty of Engineering, Chiba Univ.

Synopsis:

The CFT-PCa earthquake resistant wall structure developed for application in the construction of middle- to high-rise multi-family housing complexes consists of concrete filled tubes (CFT) columns and precast reinforced concrete (PCa RC) earthquake resistant walls. Cyclic shear bending tests were conducted on this structure using one-third scaled three-storied models which utilized two different types of connections between the columns and walls. The models of the first type, referred to as "concrete filled type" models, were constructed such that a plate girder was embedded in each wall. After the girders plates are bolted to the columns, the vertical space left between the columns and walls was filled with concrete. Models of the second type, known as "bolt type" models, were built such that each wall was embedded with a T-bar on which reinforcing bars were welded. The T-bars were then bolted to gussets fitted to the columns. Tests confirmed that both types of models demonstrate sufficient strength and energy absorption capacity. Studies of design formulas served to determine that strength can be estimated assuming such structures as an arch mechanism plus inter-story arch mechanism in the case of the concrete filled type of model and as a truss mechanism plus inter-story arch mechanism in the case of the bolt type of model structure.

1 Introduction

In recent years, there has been an increasing need for prefabricated (skeletal) frames in the field of building structures. This need has been driven by a desire to realize ever lower labour cost and shorter construction period. This has resulted in the development and application of various methods of prefabrication in the construction of multi-family housing complexes. As an example, there are many cases in which energy savings in construction work are sought through the use of precast (PCa) members in the fabrication of reinforced concrete (RC) (skeletal) frames.

In the field of composite structures, on the other hand, advances have been made in the development of mixed structures. These structures take the best advantages of both steel and concrete, and rapid progress is being made with the techniques involved with these types of structures. The use of concrete filled tubes (CFT), in particular, is considered to be becoming quite popular as a result of the superior structural performance and fire resistant qualities of such CFT structures, not to mention their ease of work.

The CFT-PCa earthquake resistant wall (shear wall) structure system combines steel girders for a direction and precast reinforced concrete shear walls (PCa shear walls for another direction) with CFT columns in the construction of middle- to high-rise multi-family housing complexes. Kawasaki Steel has developed this system because such complexes can be completed within

* Originally published in *Kawasaki Steel Giho*, **30**(1998)1, 7–13

the time period needed to fabricate steel frames when the system is industrialized. This type of system assures residents of superior comfort and habitability including stability against strong winds and insulation against sound which cannot be expected with conventional steel frame structures.

In order to clarify the fundamental strength performance of the CFT-PCa shear wall structure, cyclic shear bending tests were carried out using one-third scaled, three-story, inter-storied shear wall models. This paper describes a summary of the tests done and explores the results of an examination into the compatibility of the new system with existing shear wall design formulas based on the test results obtained.

2 Outline of Structural System

This system is an industrialized skeletal frame structure system intended for application with plate-shaped middle- to high-rise housing buildings of about 14 stories in height.

The general construction of this system consists of the use of CFT columns and the provision of PCa shear walls in the span direction. The PCa shear walls are provided with a steel framed plate girder inside without exposing the girder shape. The construction in the transverse direction consists of a rigid frame structure in which steel girders covered with concrete (SC girders) are used. This concrete covering usually serves as the first and final coats thereby eliminating the need for a separate fire-proofing covering. In order to join the SC girders to the columns, a web of the H-shaped steel used in the SC girders is bolted to the columns using high-strength bolts, and the flanges of the H-shaped steel are field-welded to the columns. The SC girders are provided with an uncovered part at each end for field-welding. After the SC girders are joined to the columns, the uncovered empty spaces at the ends of each girder are filled with slab concrete and by concreting. The PCa walls are joined to the columns by bolting the plate girders to the columns using high-strength bolts. The clearance between the PCa walls and the columns is similarly filled with slab concrete and by concreting. Concrete composite slabs are used for the floor portions of the structure, and the surface is covered with concrete in the field so that the work required for making concrete frames and for arranging the reinforced bars in the field can be reduced for improved labour cost. **Figure 1** shows the concept of the structure around the joints.

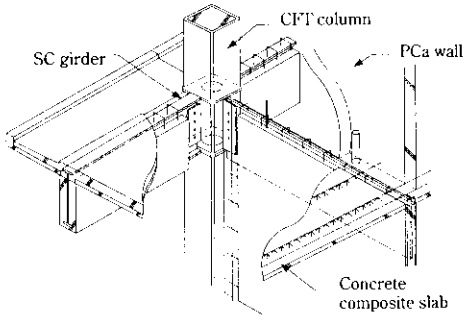

Fig. 1 Concept of CFT-PCa structure

3 Outline of Tests

3.1 Test Specimens

Test specimens were designed assuming the lower floor of a multi-story, inter-storied earthquake resistant wall and were made in a one-third scaled, three-story, one-span model. The selected test parameters consisted of the type of vertical joint used between the CFT column and PCa shear wall (**Fig. 2**), shear span ratio, and whether or not the wall has an escape hole. A total of five specimens were prepared as indicated in **Table 1**. Details of the test specimens are shown in **Fig. 3**. In the case of specimens ST10 and ST30 (bolt type), a T-bar with a welded anchor reinforcing bar was vertically embedded in the PCa panel at each end beforehand. The bar was bolted to a gusset plate welded onto the colmn using high-strength bolts. In the case of test specimens CP10, CH10 and CP30 (concrete filled type), the plate girder embedded in the PCa panel was bolted to the columns, and the vertical spaces between the panel and columns were filled with concrete without fixing the ends of the horizontal reinforcing bars of the panel.

The CH10 test specimen was provided with an opening in the panel which was assumed to be an escape hole (provided in a CP10 test specimen). Although the ST30 and CP30 test specimens have the same detailed structure as the ST10 and CP10 specimens, respectively,

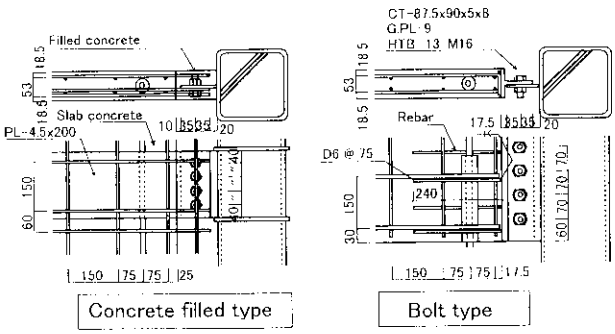

Fig. 2 Detail of joint

Table 1 List of test specimen

Name	Vertical joint	Span (mm)	
ST10	Bolt type	1 200	With hole
CP10	Concrete filled type	1 200	
CH10	Concrete filled type	1 200	
ST30	Bolt type	3 000	
CP30	Concrete filled type	3 000	

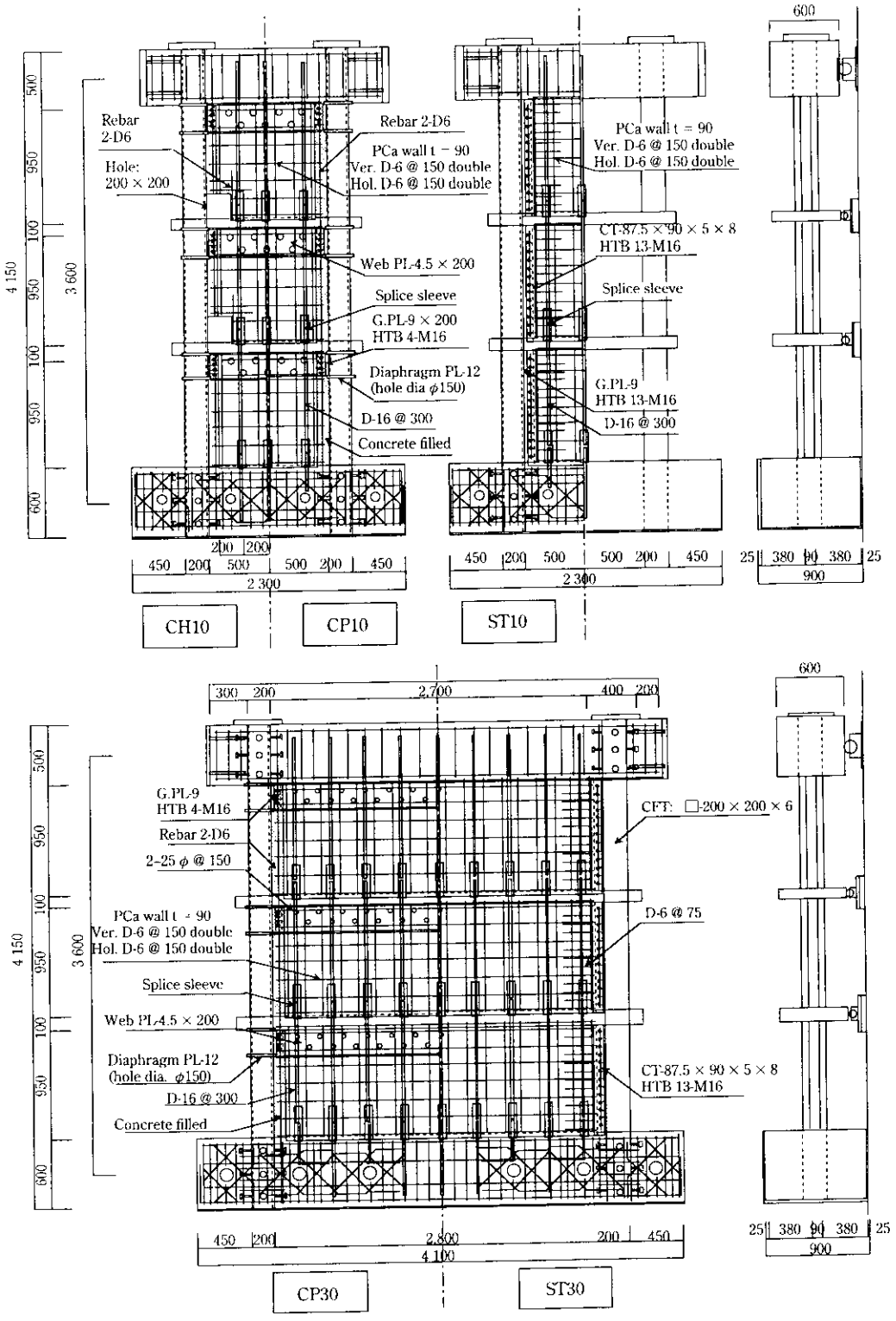

Fig. 3 Test specimen

these test specimens were assumed to be shear-fractured in the bearing wall. For all specimens, the horizontal joints between each panel and those between the panels and the floors were made by connecting the vertical joining bars of the panels using splice sleeves (cast iron pipes with a reinforcing steel bar inside) and by injecting grout into them. Installation of PCa shear panels, concrete filling of the column tubes, and concreting of the slabs and joints were done with the test specimens set in the vertical position. The mechanical properties of

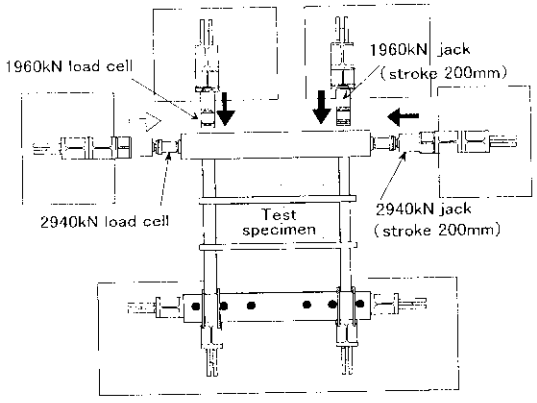

Fig. 4 Loading conditions

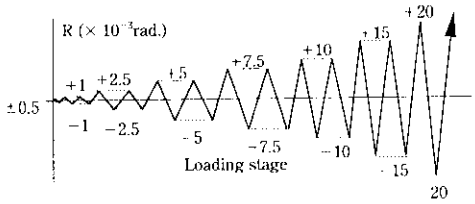

Fig. 5 Loading program

the materials used for these test specimens are described in **Tables 2** and **3**.

3.2 Method of Loading

The test specimens were place horizontally and subjected to constant axial forces (490 kN × 2) at the top part of the specimens using two sets of 2MN hydraulic jacks, as shown in **Fig. 4**. The specimens were then alternatively subjected to horizontal forces using two sets of 3MN hydraulic jacks. Loading hysteresis was controlled on the basis of the total angle of deformation as calculated from the total extent of horizontal displacement. The loads were applied in accordance with the loading program shown in **Fig. 5**.

Table 2 Material property (steel)

		YS (N/mm²)	TS (N/mm²)	YR (%)	El (%)
Column	□-200 × 6	376	460	82	32.7
CT flange	t = 8	279	434	64	29.9
CT web	t = 5	331	458	72	37.4
Plate	t = 4.5	293	451	65	38.8
Re-bar	D16	353	515	69	19.5
Re-bar	D6	453	600	76	11.0

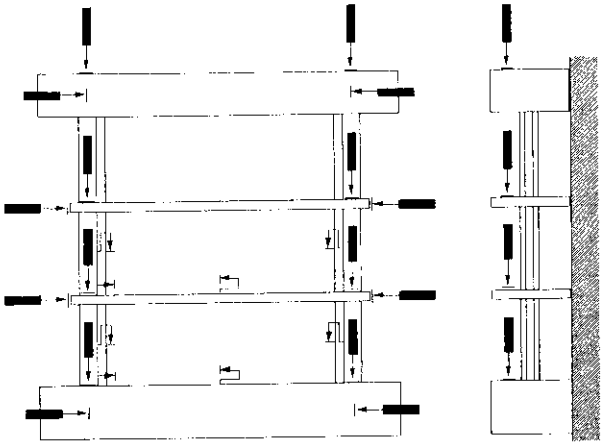

Fig. 6 Measurement of displacement

3.3 Method of Measurement

Displacement was measured for the respective horizontal and vertical displacements of each floor, as well as the degree of slip and opening of each vertical and horizontal joints as shown in **Fig. 6**. In addition to these values, the values for the strain in the column tubes, embedded plates, vertical through bars, plates used for the bolt joints, vertical reinforcing bars and horizontal reinforcing bars were measured using strain gauges.

4 Test Results

4.1 Deformation Due to Loading

The relation between horizontal load and total deformation angles as well as the condition of cracks at a deformation angle of 20×10^{-3} radians for each test specimen were shown in **Fig. 7** (a)~(e).

Table 3 Material property (concrete)

	Part	Fc (MPa)	Comp. (MPa)	Tens. (MPa)	Young's mod. (MPa)
ST10	PCa panel	23.5	32.0	2.21	—
	column, slab	35.3	34.8	2.24	—
CP10	PCa panel	23.5	31.7	2.27	—
	column, slab, joint	35.3	35.4	2.87	—
CH10	PCa panel	23.5	38.0	4.02	—
	column, slab, joint	35.3	34.0	5.30	—
ST30	PCa panel	23.5	30.0	2.28	2.22×10^4
	column, slab	35.3	33.8	2.83	2.28×10^4
CP30	PCa panel	23.5	32.3	2.36	2.20×10^4
	column, slab, joint	35.3	32.9	2.92	2.26×10^4

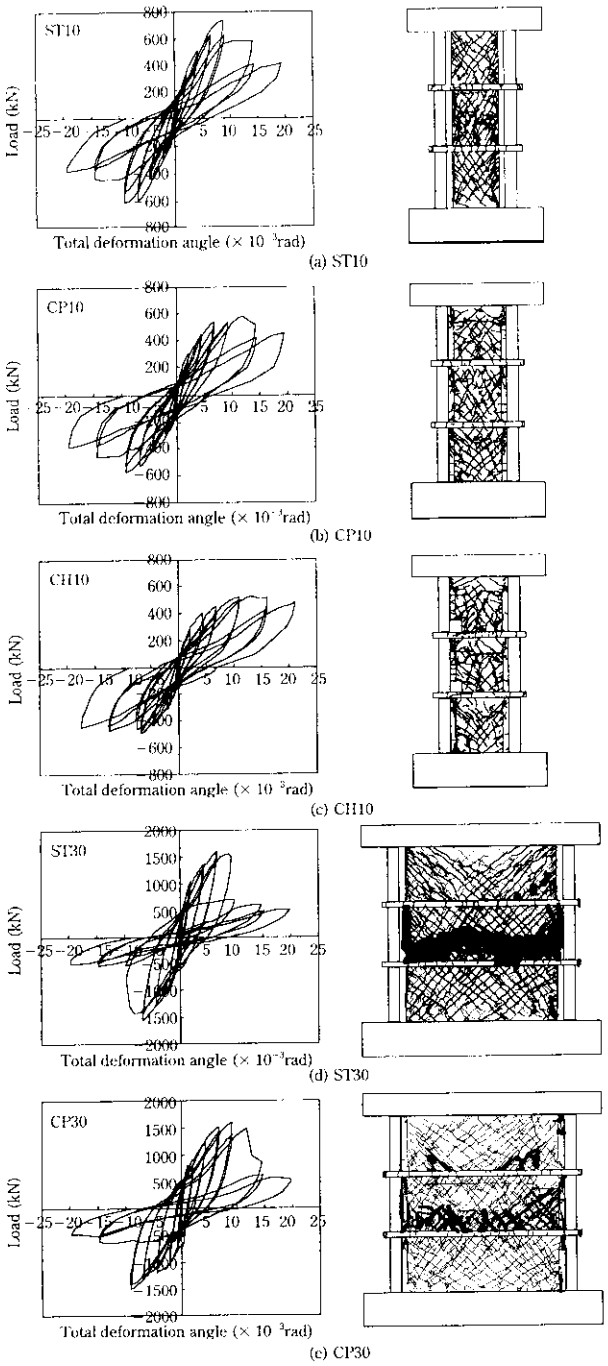

Fig. 7 Relations between load and total deformation angles and cracks

4.2 Progress of the Failure Process

(1) ST10

At the point when the deformation angle reached 2.5 $\times 10^{-3}$ radians, generation of shear cracks were observed and total stiffness also started to decrease in the vicinity of this point. Cracks propagated nearly in the 45° direction as measured against horizontal line thereafter. At the point of 5×10^{-3} radians, the anchor reinforcing bars welded on the T-bar of the second floor started to yield as a result of tension. However, the load of the structure continued to increase even beyond that point and at the point of 7.5×10^{-3} radians, tensile strain in the anchor reinforcing bars increased. At the same time, the horizontal reinforcing bars of the earthquake resistant walls yielded due to tensile stress. When the load reached the maximum in the first loop at 10×10^{-3} radians, fractures were observed at this point at several places in the anchor reinforcing bars where the material was bent or flare welded to the T-bars.

(2) CP10

At the point of 2.5×10^{-3} radians shear cracks were observed in the PC10 test specimen, and the load increased thereafter while the stiffness (of the structure) continued to decrease. At the point of 5×10^{-3} radians, surface cracks were observed at the boundary surface between the CFT columns and the filled concrete on the second floor. However, the load increased further, and the horizontal reinforcing bars and vertical joint bars of the panels on the first and second floors started to yield at the point of 10×10^{-3} radians. Thereafter, cracks were generated horizontally at the lower end of the girder plate of the third floor shear panel at a deformation angle of about 10×10^{-3} radians in the first loop at 15×10^{-3} radians. At this point, cracks were generated in the wall in such a form that the panel concrete become delaminated and the load reached its maximum value.

(3) CH10

The process of how fractures progressed in this structural model was nearly the same as that observed for the CP10 test specimen. Crack generation was observed at the point of 2.5×10^{-3} radians. Thereafter, load increased while stiffness decreased. Openings were already observed at the boundary between the CFT column and filled concrete at the point of 5×10^{-3} radians. The horizontal reinforcing bars and vertical joining bars of the panels started to yield at 7.5×10^{-3} radians, and horizontal cracks similar to those found in the CP10 structural model were generated at the lower end of the girder plate of the second floor shear panel at the point of 15×10^{-3} radians, which was also found to be the point of maximum load.

(4) ST30

Shear cracks were observed to have been generated at a deformation angle of 1×10^{-3} radians. As with the ST10 test specimen, the anchor reinforcing bars welded to the T-bar of the second floor shear panel started to yield due to tensile stress at the point of 5×10^{-3} radians. Cracks were found to be propagating in a nearly 45° angle direction as measured against the horizontal line. At the point of 7.5×10^{-3} radians, the load reached the maximum value, and althought the load remained mostly at the same level in the first

loop at 10×10^{-3} radians, it suddenly decreased thereafter and ceased to decrease at around 440 kN. At the point of maximum load, fractures were observed in the material and at the welded portions of the anchor reinforcing bars. At the same time, the horizontal reinforcing bars of the second floor panel started to yield due to tensile stress as in the case of the ST10 model.

(5) CP30

Shear cracks were observed to have formed in the CP30 test specimen at the point of 1×10^{-3} radians just as with the ST30 model. Openings were also observed at the boundary between the CFT columns and filled concrete at 5×10^{-3} radians. Thereafter, the through reinforcing bars started to yield at 7.5×10^{-3} radians, while the horizontal reinforcing bars of the second floor panel yielded. Load reached the maximum at 10×10^{-3} radians. Although load was maintained at nearly the same level until the deformation angle reached around 10×10^{-3} radians in the positive direction of the first loop at 15×10^{-3} radians, the load suddenly dropped thereafter. Cracks in the horizontal direction of the earthquake resistant panels such as those found in CP10 and CH10 were not generated in the case of the CP30 structure. After the test, concrete at the end of the girder plates was removed and the plates were confirmed to have been fractured as a result of tensile stress at the bolt holes on the ends of the girders.

For all test specimens, load ceased to decreased at around 440 kN after reaching the maximum value. The vertical joining bars did not yield until the deforrmation angle reached around 15×10^{-3} radians. Furthermore, local buckling was visually observed in the CFT columns on the compression side of the column base in the final loop at 20×10^{-3} radinas. However, this damage was relatively light.

4.3 Strain Distribution

Figure 8 shows the distribution of strain at a deformation angle of 10×10^{-3} radians in the CP10 and CP30 test specimens. From the strain distribution in the vertical joining bars and column flanges, it can be seen that although the shear panels were generally bent over the entire range, the columns tended to be increasingly bent on the compression side at the column base and were subjected to the reaction of the compression struts of the panel. This trend also appeared in the distribution of principal strain on the web portion of the column as can be seen in Fig. 8 (b).

In the case of the CP30 test specimen, the principal strain distribution in the girder plate indicates a condition of pure tension which also corresponds to the fracture condition observed after disassembly of the specimen. In the case of the CP10 test specimen, on the other hand, strains were not in one direction due to the effect of exposure bending. It may be presumed that the girder

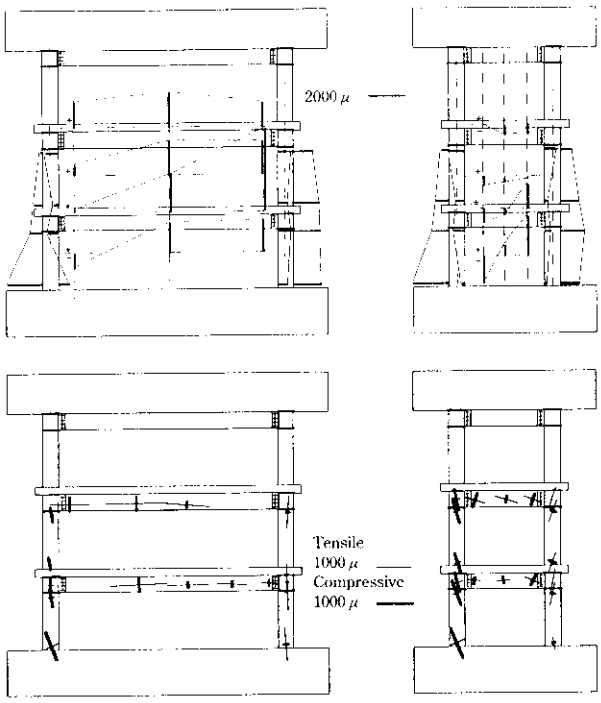

(a) CP30 (b) CP10

Fig. 8 Strains and principal strains at 1/100

plate buckled as a whole as the result of exposure bending. This, in turn, led to the panel becoming subjected to a shearing force from inside in the direction perpendicular to the panel surface at the position of the girder plate, with fracturing occurring at the position of the lower end of the girder plate. However, the fracture mechanism has not been clarified and further detailed studies are needed in order to better understand the mechanism involved.

4.4 Behavior of Joining Parts

4.4.1 Deformation of openings

Figure 9 shows the relationship between total deformation angle and displacement of the opening measured at the base of the columns at the first and second floors. This figure indicates that the behavior with respect to the first and second floors in the stage of little deformation up to about 2.5×10^{-3} radians in the total deformation angle was almost identical for both floors and no openings appeared. However, it is presumed that openings started to appear on the second floor from a total deformation angle of about 5×10^{-3} radians. No clear openings appeared on the first floor until the load nearly reached the maximum value. Displacement of the opening on the second floor appeared under both positive load and negative load. This observation is presumed to be due to the opening having been made while under positive load when the column was subjected to tension and remaining even when the load was changed to negative. The degree of opening was larger in the

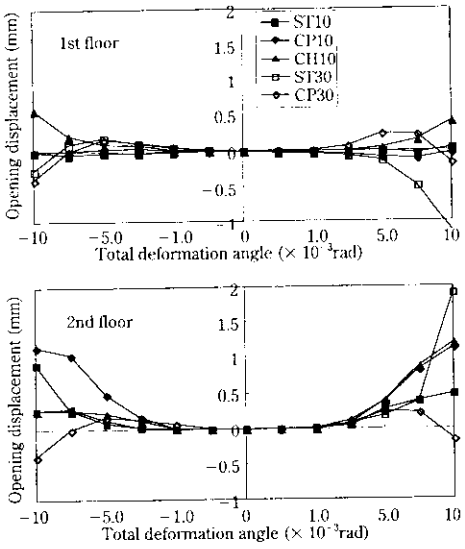

Fig. 9 Opening displacement of vertical joint

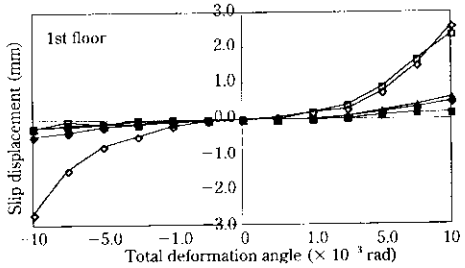

Fig. 10 Slip displacement of horizontal joint

concrete filled type specimens than in those of the bolt type. This tendency was particularly evident in the 10-series test specimens.

4.4.2 Slip deformation

Figure 10 shows the relationship between horizontal slip displacement at the lower end of the panel on the first floor and the total deformaion angle. According to this figure, it is considered that almost no slip deformation occurred in the horizontal direction in the case of the 10-series test specimens. However, slip displacement started to occur from a total deformation angle of about 5×10^{-3} radians in the case of the 30-series test specimens.

Figure 11 shows the relationship between vertical place displacement at the vertical joints on the second floor and the total deformation angle. Slip displacement was found to be greater in the case of the concrete filled type specimens than in the case of bolt type specimens.

4.5 Equivalent Damping Characteristics

Figure 12 shows the equivalent damping factor for each hysteresis loop of each test specimen. The average of the values in the positive and negative directions were

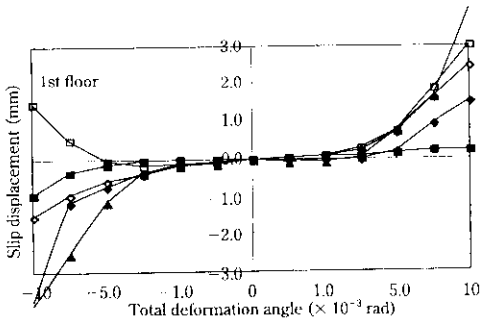

Fig. 11 Slip displacement of vertical joint

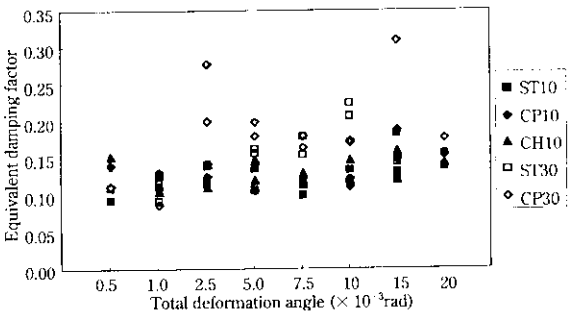

Fig. 12 Equivalent damping factor

used to determine equivalent potential energy.

The figure shows that damping was relatively large for the 30-series test specimens, being 0.15~0.25 in terms of the equivalent damping factor. This factor was around 0.10~0.15 for the 10-series test specimens. These values are rather high compared with the date[1] obtained for the RC earthquake resistant walls in the past. Further, the energy absorption capacity of the PCa shear walls can be regarded as being high.

5 Examination of Design Formulas

5.1 Initial Stiffness and Cracking Strength

Table 4 shows the calculated values for initial stiffness and cracking strength obtained using Eqs. (1) and (2), respectively. The experimental values for stiffness were determined from the relation between the gradient of the load and deformation for the first loop as obtained

Table 4 Initial stiffness and cracking strength

	Initial stiffness			Cracking strength Qscr (kN)
	Exp. (kN/cm)	Cal. (kN/cm)	Exp. Cal.	
ST10	666	874	0.76	198
CP10	689	873	0.79	197
CH10	698	897	0.78	216
ST30	4 421	4 226	1.05	537
CP30	3 918	4 320	0.91	558

by least square approximation. Although scattering in a wide range, it can be said that the calculated values for initial stiffness are in close agreement with the test values.

The calculated values for shear cracking strength nearly correspond to the points of bending on the curves plotting the total deformation angle against load according to the tests.

$$Ks = Aw \cdot G/(\chi \cdot h),\quad Kb = 3Ec \cdot Ie/h^3$$

$$Kwl = 1/(1/Ks + 1/Kb) \cdots\cdots (1)$$

$$Qscr = 37.6\sqrt{Fc} \cdot \{1 + n/2 \cdot (ph + pv)\}t \cdot l \cdots (2)$$

where

Aw: Sectional area of wall (cm^2)
G: Shear stiffness
χ: 1.2
h: Height of wall
t: Thickness of wall
l: Inside length of wall
n: Ratio of Young's modulus
Ec: Young's modulus for concrete
Ie: Equivalent geometrical moment of inertia taking reinforcing bars of wall into account (cm^4)
Kwl: Initial stiffness
Qscr: Cracking strength (N)
ph: Ratio of horizontal reinforcing bar
pv: Ratio of vertical reinforcing bar
Fc: Design standard strength of concrete (N/mm^2)

5.2 Maximum Strength

The maximum strength obtained from the tests and those obtained by calculation are shown in **Table 5**. The calculated values (1) and (2) are those based on the Standard for Structural Calculation of SRC Structures[2], while those according to the Design Guidelines for Earthquake Resistant RC Buildings. Based on Ultimate Strength Concept[3], respectively. The calculated values (3) and (4) are those obtained through the use of strength formulas which are taking the effects of multi-story construction. The calculated values (3) were calculated on the basis of the method reported in the literature[4]. The calculated values (2)–(4) are based on the ultimate strength concept (truss action and arch action). In applying this concept to CFT columns, the effect of the side columns was calculated using Eq. (3) taking the correlation between axial force and bending moment of CFT columns into account.

$$\begin{aligned} Mcu &= [\sigma cy - \{Ncc - Fcc \cdot Ac(1 - psc) \\ &\quad - \sigma cy \cdot Ac \cdot psc/2\}/(tc \cdot Dc)] \cdot tc \cdot Dc(tc - Dc) \\ &\quad (\text{when } Ncc \geqq Fcc \cdot Ac(1 - psc) \\ &\quad + \sigma cy \cdot Ac \cdot psc/2) \\ &= \sigma cy \cdot tc \cdot Dc(Dc - tc) \\ &\quad + \sigma cy \cdot tc \cdot [(Dc - 2 \cdot tc)^2 \\ &\quad - [\{Ncc - Fcc \cdot Ac(1 - psc)\}/\sigma cy/2tc]^2]/2 \\ &\quad (\text{when } (Fcc \cdot Ac(1 - psc) < Ncc \\ &\quad \leqq Fcc \cdot Ac(1 - psc) + \sigma cy \cdot Ac \cdot psc/2) \\ &= \sigma cy \cdot Zcu \ (\text{when } Ncc \leqq Fcc \cdot Ac(1 - \cdot psc)) \end{aligned} \cdots\cdots (3)$$

The calculated values (4) were obtained assuming that an inter-story arch mechanism works between the base and top of the three-story earthquake resistant wall. In addition, the ST-series test specimens were regarded as consisting of a truss structure plus, inter-story arch structure, while those of the CP-series were regarded as being of a between-floor arch mechanism plus, inter-story arch mechanism (**Fig. 13**). It was assumed that the shearing force borne by the between-floor arch mechanism balanced (counteracted) the tensile force of the plate girder. The reason for this is because in the case of the test done on the CP-series specimens, opening were generated even when the vertical joints on the second floor were in a compressed condition. Therefore, it was considered that no restrictive reaction from the columns other than those on the first floor could be expected. However, in the case of the multi-story, inter-story arch mechanism assumed in the calculated values (4), the effective length of the wall was increased considering the restrictive reaction on the top portion of the columns on the loading side against the wall, on the assumption

Table 5 Experimental result and calculation of maximum strength

(Unit: kN)

Test Specimen		Exp.	Cal. (1)	Cal. (2)	Cal. (3)	Cal. (4)	Exp./Cal. (1)	Exp./Cal. (2)	Exp./Cal. (3)	Exp./Cal. (4)
ST10	+	733	574	635	434	615	1.28	1.15	1.69	1.19
	−	609					1.06	0.96	1.40	0.99
CP10	+	580	571	572	468	584	1.01	1.01	1.24	0.99
	−	576					1.01	1.01	1.23	0.99
CH10	+	524	504	510	403	503	1.04	1.03	1.30	1.04
	−	497					0.99	0.98	1.23	0.99
ST30	+	1 592	1 556	1 700	1 386	1 687	1.02	0.94	1.15	0.94
	−	1 563					1.00	0.92	1.13	0.93
CP30	+	1 592	1 614	1 620	1 380	1 513	0.99	0.98	1.15	1.05
	−	1 492					0.92	0.92	1.08	0.99
						Ave.	1.03	0.99	1.26	1.01
						Var. (%)	0.8	0.4	2.8	0.5

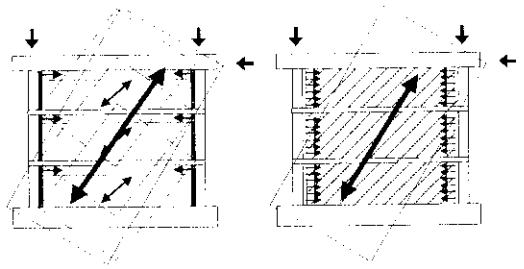

(a) Arch action and inter-story arch action for CP, CH specimen (b) Truss action and inter-story arch action for ST specimen

Fig. 13 Assumed mechanism for cal. (4)

that the effective factor of the compression strength of concrete does not decrease due to the guaranteed deformation angle and that the loading girders are strong. The calculated values for the CH-series test specimens represnt the results obtained by multiplying the results equally according to the respective methods of calculation by the strength reduction factor given in the Standard for SRC Structures. Direction was not taken into account in these calculations. The effect of the slab reinforcing bars was not taken into consideration either.

It may be said that all calculated values nearly correspond to the test results with the exception that the calculated values (3) are somewhat low. The calculated values (2) tend to be on the high side for the ST-series test specimens on which truss mechanism works, particularly for those of the 30-series which have a small shear span ratio. However, this is presumably because the angle of the truss mechanism is fixed at 45°.

Nevertheless, no consideration could be taken into these calculated values with respect to the phenomenon of delamination cracks being generated horizontally in the concrete in the CP10 and CH10 test specimens at the position of the girder plate. Further, the maximum yield strength for these structures was reached. However, from the fact that the load level was such that the average shearing stress increased up to about 20% of compression strength of wall concrete, the calculated values can be approved as being fairly appropriate for use in estimating the strength of the shear wall.

The details of each calculation formula are in accordance with Eqs. (4)–(8). Symbols not specifically noted are those formulas given in the original literatures.

- Calculated Values (1): According to the Standard for Structural Calculation of Steel Reinforced Concrete Structures of the Architectural Institute of Japan.

$$wQu = r \cdot \min\{wF's, (wp \cdot w\sigma y + w\tau u)\}tw \cdot l' \cdots (4)$$

- Calculated Values (2): According to the Design Guidelines for Earthquake Resistant Reinforced Concrete Buildings Based on the Ultimate Strength Concept of the Architectural Institute of Japan.

$$Vu = tw \cdot lwb \cdot ps \cdot \sigma sy \cdot \cot\phi + \tan\theta(1-\beta)tw \cdot lwa \cdot \nu Fc/2 \cdots\cdots\cdots (5)$$

$$lwa = l' + Dc + \Delta lwa,$$

$$\Delta lwa = 1/\cos\theta \cdot \sqrt{[2 \cdot Mcu/\{\nu Fc \cdot tw \cdot (1-\beta)\}]}$$

$$lwb = l' + Dc + \Delta lwb, \quad \Delta lwb = Dc$$

$$\tan\theta = \sqrt{\{(hw/lwa)^2 + 1\}} - hw/lwa, \quad \cot\phi = 1.0$$

$$\nu_0 = 0.7 - Fc/2\,000,$$

$$\nu = (1.2 - 40\,Ru)\nu_0, \quad Ru = 0.01$$

- Calculated Values (3): Naganuma's equation (formula)

$$Vu = tw \cdot lwb \cdot pshe \cdot \sigma sy \cdot \cot\phi + \tan\theta(1-\beta)tw \cdot lwa \cdot \alpha_1 \cdot \alpha_2 \nu Fc/2 \cdots (6)$$

$$\Delta lwa = l' + Dc + \Delta lwa,$$

$$lwa = 1/\cos\theta \cdot \sqrt{[2 \cdot Mcu/\{\nu Fc \cdot tw \cdot (1-\beta)\}]}$$

$$\tan\theta = \sqrt{\{(h/lwa)^2 + 1\}} - h/lwa, \quad \cot\phi = 1.0$$

$$pshe = psh + Ab/(tw \cdot hw) \cdot \sigma by/\sigma sy,$$

$$psve = psv + 2psc \cdot Ac/(tw \cdot l)$$

$$\beta = (1 + \cot^2\phi)pshe \cdot \sigma sy/(\alpha_1 \cdot \alpha_2 \nu Fc)$$

$$\alpha_1 = 1.04 + 0.06 \cdot h/l - (0.4 \cdot h/l + 0.16)/(100 \cdot psve)$$

$$\alpha_2 = 1.20 - 0.14 \cdot h/l \quad (h/l < 1.40)$$

$$= 1.00 \quad (h/l \geqq 1.40)$$

where

Ab: Sectional area of girder plate

α_1: Correction factor for effective strength depending on equivalent vertical reinforcing bar ratio

α_2: Correcting factor for effective strength depending on method of how force is applied

- Calculated Values (4): Proposed equation (formula)

Cp-series: Between-floor arch mechanism + multi-story, inter-story arch mechnism

$$Vu = \gamma \cdot tw \cdot lwc \cdot \nu Fc/2 + \tan\theta_2(1+\gamma)tw \cdot lwa \cdot \nu Fc/2 \cdots\cdots\cdots (7)$$

$$lwa = l' + Dc + \Delta lwa + \Delta lwa', \quad lwc = l' + 2Dc$$

$$\Delta lwa = 1/\cos\theta_2 \cdot \sqrt{[2 \cdot Mcu/\{\nu Fc \cdot tw \cdot (1-\gamma)\}]}$$

$$\tan\theta_2 = \sqrt{\{(h/lwa)^2 + 1\}} - h/lwa,$$

$$\gamma = 2Ab \cdot \sigma by/(tw \cdot lwc \cdot \nu Fc)$$

where

lwa: Equivalent wall length of inter-story arch mechanism

lwc: Equivalent wall length of between-floor arch mechanism

Δlwa: Increment (change in) equivalent wall length of inter-story arch mechanism at the column top on the compression side

Δlwa': Increment (change in) equivalent wall length of inter-story arch mechanism at the column top on the tension side

γ: Load bearing ratio of multi-story, inter-story arch structure with respect to the between-floor arch structure

$\tan\theta_2$: Angle of compression bundle of inter-story arch mechanism

Mcu: Bending strength taking axial force of col-

umn into consideration
Ab: Sectional area of girder
$\sigma$by: Yield strength of girder
ST-series: Truss mechanism + multi-story, inter-story arch mechanism

$$Vu = tw \cdot lwb \cdot ps \cdot \sigma sy \cdot \cot\phi + \tan\theta_2(1-\beta)tw \cdot lwa \cdot \nu Fc/2 \quad \cdots\cdots\cdots (8)$$

$$\tan\theta_2 = \sqrt{\{(h/lwa)^2 + 1\}} - h/lwa, \quad \cot\phi = 1$$

$$lwa = l' + Dc + \Delta lwa + \Delta lwa',$$

$$lwb = l' + Dc + \Delta lwb$$

6 Conclusion

Shear bending tests were performed on the CFT-PCa earthquake resistant wall (shear wall) structure (for five different types of test specimens). The following points became clarified as a result of these tests.

(1) In the case of both the concrete filled type and the bolt type structures, the shear wall was found to have excellent yield strength and energy absorption capacity until shear fracturing occured at a total deformation angle of about 10×10^{-3} radians.

(2) The initial stiffness and cracking strength for both types of structures could be calculated using existing formulas regardless of the method of joining used.

(3) Maximum strength can be accurately estimated using the calculation formulas assuming an between-floor arch mechanism and inter-story arch mechanism even for the concrete filled type of wall structure.

(4) There is some possibility that with plate girders of a short span, the wall will fracture horizontally due to lateral buckling of the plate.

From the test results, it could be confirmed that the capacity of CFT-PCa structures is basically fully adequate for practical application. We are planning to continue our studies into ways how to improve and realize commercial construction of this structure.

References

1) Japan Institute of Construction Engineering: "Ministry of Construction—General Technology Development Project, Development of Technology for Super Lightweight, Super High-Rise Reinforced Concrete Buildings, Report of Structural Capacity Working Group", (1993)

2) Architectural Institute of Japan: "Standard for Structural Calculation of Steel Reinforced Concrete Structures", (1987)

3) Architectural Institute of Japan: "Design Guidelines for Earthquake Resistant Reinforced Concrete Buildings Based on Ultimate Strength Concept", (1990)

4) K. Naganuma: "Study on Non-Linear Analytical Method and Shear Strength of Resistant Reinforced Concrete Wall", Doctor Paper in Chiba Univ., (1993)